

13th International Conference on Greenhouse Gas Control Technologies, GHGT-13, 14-18 November 2016, Lausanne, Switzerland

## Modelling the adsorption-desorption behavior of CO<sub>2</sub> in shales for permanent storage of CO<sub>2</sub> and enhanced hydrocarbon extraction

Solomon Brown<sup>a\*</sup>, Greeshma Gadikota<sup>b</sup> and Niall Mac Dowell<sup>c</sup>

<sup>a</sup>Department of Chemical and Biological Engineering, The University of Sheffield, UK

<sup>b</sup>Department of Civil and Environmental Engineering, Princeton University, New Jersey, USA

<sup>c</sup>Centre for Process Systems Engineering, Imperial College London, UK

### Abstract

Increasing global need for energy security has spurred a need for enhanced oil and gas recovery from unconventional reservoirs. From a carbon cycle point of view however, enhanced hydrocarbon extraction results in higher concentrations of CO<sub>2</sub> in the atmosphere, which is detrimental to the environment. Coupling the potential of storing CO<sub>2</sub> with gas and oil recovery is one approach to limit the rise in atmospheric CO<sub>2</sub> concentrations while allowing for subsurface hydrocarbon recovery. Over the past few years, shale gas and oil have emerged as one of the leading contributors to overall subsurface hydrocarbon recovery. In this study, we explore the potential of combining the adsorption of CO<sub>2</sub> with the enhanced recovery of CH<sub>4</sub>, and compare the results with water which is conventionally used for hydraulic fracturing. The adsorption-desorption behaviour is accounted for using published experimental Langmuir isotherm data. The model assumes a simplified fracture shape where the flow is one-dimensional and Darcy's law is obeyed. Key performance indicators include tonnes of CO<sub>2</sub> injected per scm CH<sub>4</sub> recovered, tonnes of H<sub>2</sub>O injected per scm CH<sub>4</sub> recovered and tonnes of CO<sub>2</sub> sequestered per tonne of CO<sub>2</sub> injected.

© 2017 The Authors. Published by Elsevier Ltd. This is an open access article under the CC BY-NC-ND license (<http://creativecommons.org/licenses/by-nc-nd/4.0/>).

Peer-review under responsibility of the organizing committee of GHGT-13.

*Keywords:*

### Nomenclature

|        |  |
|--------|--|
| $\phi$ | Rock porosity (volume of voids per total volume) |
|--------|--|

\* Corresponding author. Tel.: +44 1142227597

E-mail address: [s.f.brown@sheffield.ac.uk](mailto:s.f.brown@sheffield.ac.uk)

|                       |   |
|-----------------------|---|
| $S_g$                 | gas saturation (volume of gas per volume of voids)                                  |
| $\rho^b$ :            | bulk free gas density (mass of gas per volume of gas)                               |
| $\rho^a$ :            | absorbed gas density (mass of absorbed gas per total volume of rock)                |
| $\kappa$ :            | effective permeability (relative permeability multiplied by intrinsic permeability) |
| $\mu^b$               | the bulk gas viscosity  |
| $p$                   | pore gas pressure   |
| $\omega_c$            | mass fraction of $\text{CO}_2$  |
| $\rho_c^a$            | absorbed density of $\text{CO}_2$   |
| $\rho_m^a$            | absorbed density of $\text{CH}_4$   |
| $D_c$                 | $\text{CO}_2$ dispersion coefficient  |
| $u^b$                 | Darcy flux of bulk gas phase  |
| $n$                   | amount of gas absorbed (mol or mass)  |
| $n^{\max}$            | max amount of gas that can be absorbed (mol or mass)                                |
| $K$                   | Langmuir Constant   |
| $n_1$                 | amount of component 1 absorbed in binary system (mass or mol)                       |
| $n^e$                 | excess amount absorbed  |
| $n^{\text{abs}}$      | absolute amount absorbed  |
| $V_a$                 | volume of pore space occupied by absorbed phase                                     |
| $\rho_1^e$            | excess absorbed mass of component 1 per unit volume of rock                         |
| $\rho^b$              | Bulk gas density  |
| $\rho_a$              | absorbed phase density  |
| $\omega_1^a$          | absorbed mass fraction component 1  |
| $\rho_1^{\text{abs}}$ | component 1 absolute absorption   |
| $d$                   | distance between adjacent hydraulic fractures                                       |
| $n^f$                 | number of hydraulic fractures   |
| $a_f$                 | surface area of each hydraulic fracture plane                                       |

## 1. Introduction

Natural gas contained within shale formations represent a significant energy reserve, which has only begun to be exploited at very large scale in the last decade. This delay is due in large part to the extremely low permeability of these geological structures, which prohibits conventional hydrocarbon extraction methods. In order to increase the permeability, and thereby increase production to economic levels, the formation is ‘stimulated’ by hydraulic fracturing of the rock. Currently, given its low cost and availability, water is used as the main constituent of the fracturing fluid in over 95 % of operations [4], typically mixed with proppant, surfactants and biocide.

In recent years however, due to the issues related to the use of water, not least the amounts volumes required, attention has turned to finding alternative fracturing fluids.  $\text{CO}_2$  is one such substitute [9], which has long been used in hydrocarbon production through Enhanced Oil Recovery [5]. This is because of  $\text{CO}_2$ s greater miscibility with hydrocarbons and enhanced desorption of  $\text{CH}_4$  from the clays that make up the shale formations that may lead to greater gas production.

Furthermore, given the current need to reduce the amount of  $\text{CO}_2$  release to the atmosphere and limit climate change, the possibility for storage of the injected  $\text{CO}_2$  in shale wells while also potentially enhancing hydrocarbon production is of interest. Work on predicting the impact of the use of  $\text{CO}_2$  on production has been presented in the literature, the models applied are complex fluid dynamic simulations [3] or assessments based on isotherms and empirical correlations [12]; the former of these methods requires significant computational power and is therefore not suited to a process level assessment, while the latter cannot be readily extended to account for more complex scenarios. The analysis of shale production performed by Patzek et al. [10,11] has shown that a simplified one-dimensional model can be used to characterise the flow within a shale reservoir; such a model provides a firm basis on which to base a process assessment of the injection and production of a shale well. Indeed, the model suggested by Patzek et al. [10,11] has been used by Edwards et al. [2] to predict the injectivity and capacity of depleted shale gas wells in the US.

In this work we develop a rigorous process level model to assess both the increased potential for production of natural gas from shale formations when CO<sub>2</sub> is used a fracturing fluid as compared to water and the degree of sequestration of the CO<sub>2</sub>. The paper proceeds as follows: Section 2 presents the flow model along with the boundary conditions applied for the fracturing scenarios as well as the adsorption, transport and thermophysical models. Section 3 presents the application of this model to the hydraulic fracturing of two differing formations, in each case the effect on production and degree of carbon sequestration is investigated. Finally, conclusions are drawn in Section 4.

## 2. Methodology

### 2.1. Fluid flow model

In order to model the flow of CO<sub>2</sub> and natural gas within the porous rock structure of the Shale reservoir we follow and describe the fluid behaviour as a single-phase, isothermal, one-dimensional Darcy diffusional flow [1,11]. Figure 1 presents the assumed geometry of the shale gas reservoir, a horizontal well with perforations at regular intervals. It is further assumed that the permeability in the fracture and in the well is effectively infinite.

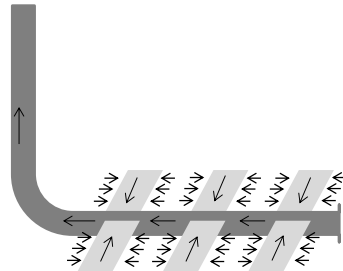


Fig. 1. Schematic representation of the assumed reservoir geometry

The conservation of mass of the fluid mixture along with the assumption of Darcy flow can be written as the following non-linear diffusion equation, and given that the flow is isothermal this is a function of only the pressure:

$$\frac{\partial}{\partial t} [\phi S_g \rho^b(p) + \rho^a(p)] - \frac{\partial}{\partial x} \left( \frac{\kappa \rho^b(p)}{\mu^b(p)} \frac{\partial p}{\partial x} \right) = 0 \quad (1)$$

In order to apply the above equation to a mixture of CO<sub>2</sub> and natural gas within the bulk, Equation 1 is written in terms of the individual components, as follows:

$$\frac{\partial}{\partial t} [\phi S_g \rho^b(\omega_c, p) + \rho_c^a(\omega_c, p) + \rho_m^a(\omega_c, p)] - \frac{\partial}{\partial x} \left[ \frac{\kappa \rho^b(\omega_c, p)}{\mu^b(\omega_c, p)} \frac{\partial p}{\partial x} \right] = 0 \quad (2)$$

Further, an additional transport equation is solved to account for the flow of CO<sub>2</sub> within the bulk fluid:

$$\begin{aligned} \frac{\partial}{\partial t} [\phi S_g \rho^b(\omega_c, p) \omega_c + \rho_c^a(\omega_c, p)] + \frac{\partial}{\partial x} [\rho^b(\omega_c, p) u^b \omega_c] - \\ \frac{\partial}{\partial x} \left[ \phi S_g \rho^b(\omega_c, p) D_c \frac{\partial \omega_c}{\partial x} \right] = 0 \end{aligned} \quad (3)$$

In Equation 3, the Darcy flux of the bulk gas phase is defined as follows:

$$u^b = -\frac{\kappa}{\mu^b(\omega_c, p)} \frac{\partial p}{\partial x} \quad (4)$$

The model is then closed using the additional relation:

$$\omega_c + \omega_m = 1 \quad (5)$$

## 2.2. Adsorption-desorption

The sorption behavior of CH<sub>4</sub> and CO<sub>2</sub> in porous media has been well described by the Langmuir adsorption model [6]. The Langmuir function describes the absolute amount of gas adsorbed to the media, for a two component mixture where the components are competing for the adsorption sites. The Langmuir model used to compute the adsorption for each component is given by:

$$n_i = n_i^{\max} \frac{K_i p_i}{1 + K_1 p_1 + K_2 p_2} \quad (6)$$

Following [1][6] to account for the free gas within the porous structure that is not adsorbed to the surface we define the excess adsorption by:

$$n_l = n^{\text{abs}} - V_a \rho^b \quad (7)$$

The above Langmuir isotherm can be used to estimate the excess adsorption, assuming that the parameters describe the absolute adsorption, as follows:

$$\rho_l^e = \rho_l^{\max} \frac{K_1 p_1}{1 + K_1 p_1 + K_2 p_2} \left( 1 - \frac{\omega_l \rho^b(\omega_l, p)}{\omega_l^a(\omega_l, p) \rho_a} \right) \quad (8)$$

The adsorbed mass fraction of component  $i$  can then be defined as:

$$\omega_l^a = \frac{\rho_l^{\text{abs}}(\omega_l, p)}{\rho_l^{\text{abs}}(\omega_l, p) + \rho_2^{\text{abs}}(\omega_l, p)}, \quad i = 1, 2 \quad (9)$$

Furthermore, for the purposes of the simulations carried out in this work the volume adjusted Peng-Robinson [8,13] is applied to predict the thermodynamic properties of the mixture for the CH<sub>4</sub>, CO<sub>2</sub> and H<sub>2</sub>O, while the mixture viscosity is obtained using the Refprop database [8].

## 2.3. Initial and Boundary conditions

In this work, we assume that the reservoir is initially equilibrated with a given reservoir pressure containing natural gas, represented by CH<sub>4</sub> with a trace (0.1 wt%) amount of CO<sub>2</sub>.

The domain of each simulation is taken as the half-length between each fracture (see Fig. 1), in order to close the above flow model we develop appropriate initial and boundary conditions. For the boundary midway between fractures, a Neumann condition is applied for both equations 2 and 3. At the fracture face of the other boundary, we describe the initial injection of CO<sub>2</sub> to create the fracture followed by the production of gas using a time dependent boundary condition for the two phases in the following section:

### 2.3.1. Injection phase

It is assumed that the pressure at the fracture phase is gradually increased to a level of 10 MPa ( $P_{injection}$ ) above the reservoir pressure, which for the sake of this work represents a reasonable level at which a fracture may be opened [7]. In this work this period, is represented by  $t_{injection}$  is 3 days, which is small relative to the time-scales of the dynamics involved. Further assuming that this increase in pressure is linear, for  $t \leq t_{injection}$  the boundary pressure is given by:

$$P_{boundary} = P_{reservoir} + P_{injection} \frac{t}{t_{injection}} \quad (10)$$

Given that during this period the CO<sub>2</sub> is being injected the condition for equation 3 is simply:

$$\omega_{c,boundary} = 1 \quad (11)$$

### 2.3.2. Production phase

During the production phase of operation, i.e.  $t > t_{injection}$ , it is assumed that the pressure drops below the reservoir pressure to a production pressure, here assumed to be  $P_{boundary} = 3.5$  MPa, while a Neumann condition is applied to equation 3:

$$\frac{\partial \omega_{c,boundary}}{\partial x} = 0 \quad (12)$$

## 3. Results and Discussion

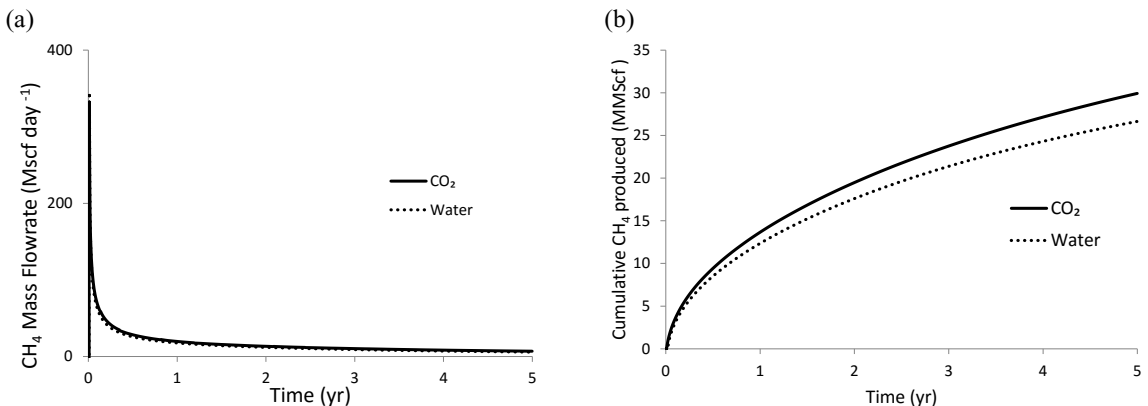
The following presents the application of the model described above to simulate the impact of the use of CO<sub>2</sub> as a fracturing fluid for hydraulic fracturing. For this purpose we use the formation parameters of the Marcellus Average and Barnett average formations obtained by Edwards et al. [1,2] by history matching against data for those formations. Table 1 presents the adsorption parameters, reservoir properties and assumed fracture geometry in each of these two cases. The simulations are performed for the domain between one axisymmetric fracture and midway point to the next, as shown in Figure 1. The wells are made up of a number of such fractures and the results are scaled accordingly.

Figures 1 (a) and (b) represent the variation of the production rate and the cumulative mass of CH<sub>4</sub> with time in the case of Marcellus Average Scenario, both where CO<sub>2</sub> and water are used, respectively. Similar results are presented in Figures 2 (a) and (b) for the Barnett Average scenario.

As may be observed in Figure 1 while the production rate using the water is initially slightly higher (see Figure 1(a)) throughout the remainder of the simulation, the flowrate is slightly higher where CO<sub>2</sub> is used. This results in an increased production of CH<sub>4</sub> over the lifetime of the simulation of approximately 10%. The same trends are observed in the case of the Barnett Average scenario, though the flowrates are slightly lower due to the properties of the respective formation.

Table 1. Shale formation and fluid properties [1]

|   | Marcellus Average | Barnett Average |
|---|-------------------|-----------------|
| <b>Adsorption properties</b>                          |                   |                 |
| CH <sub>4</sub> Langmuir K (MPa)                      | 0.17              | 0.17            |
| CO <sub>2</sub> Langmuir K (MPa)                      | 0.1               | 0.1             |
| Max. CH <sub>4</sub> Adsorption (kg m <sup>-3</sup> ) | 6.5               | 5               |
| Max. CO <sub>2</sub> Adsorption (kg m <sup>-3</sup> ) | 5                 | 45              |
| Adsorbed Phase density                                | 1000              | 1000            |
| <b>Reservoir Properties</b>                           |                   |                 |
| Effective Permeability (nD)                           | 25                | 45              |
| Gas Saturation %                                      | 75                | 75              |
| Porosity %  | 6                 | 6               |
| Reservoir Pressure (MPa)                              | 25                | 35              |
| <b>Fracture properties</b>                            |                   |                 |
| Fracture Height, V (m)                                | 32                | 32              |
| Fracture Width, H (m)                                 | 200               | 200             |
| Half spacing between fractures (m)                    | 15                | 15              |

Fig. 1 Variation of the (a) production rate (b) cumulative mass of CH<sub>4</sub> produced with time from a single fracture using CO<sub>2</sub> and Water as the fracturing fluid respectively for the Marcellus scenario.

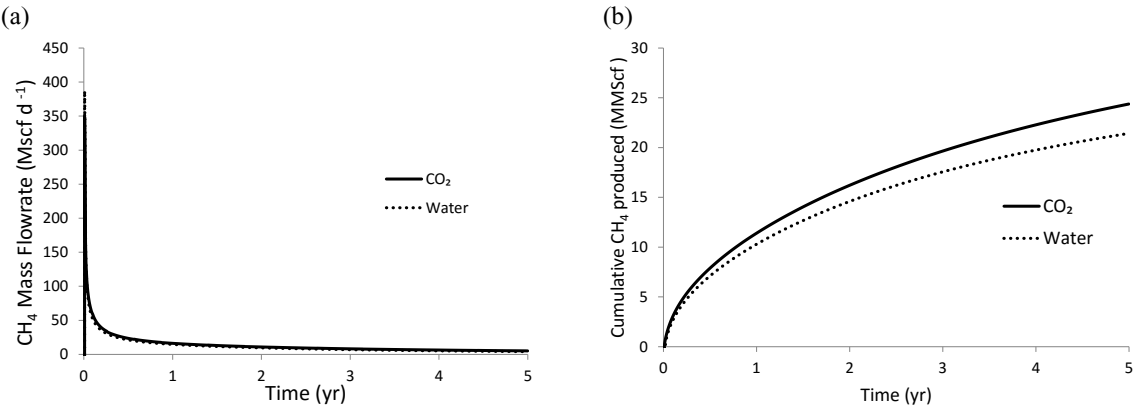


Fig. 2 Variation of the (a) production rate (b) cumulative mass of CH<sub>4</sub> produced with time from a single fracture using CO<sub>2</sub> and Water as the fracturing fluid respectively for the Barnett scenario.

Table 2 presents the performance indicators used for these scenario, i.e. the amount of CH<sub>4</sub> recovered per amount of fracturing fluid injected into the reservoir. As can be seen, for both the Marcellus and Barnett cases the amount of CH<sub>4</sub> recovered is five times greater per tonne of CO<sub>2</sub> than is the case of water.

Table 2. Comparison of production over 5 years of simulation

|  | Marcellus Average | Barnett Average |
|--|-------------------|-----------------|
| CH <sub>4</sub> recovered (MMscf/tonne CO <sub>2</sub> ) | 2.79              | 1.38            |
| CH <sub>4</sub> recovered (MMscf/tonne Water)            | 2.48              | 1.06            |

#### 4. Conclusion

In this work, a process level modelling approach is used to describe the competitive adsorption and desorption behaviour of CO<sub>2</sub> and CH<sub>4</sub> for enhanced gas recovery. This model serves as a means to assess the effect of substituting CO<sub>2</sub> as a fracturing fluid for the enhanced recovery of gas from geologic formations with pore spaces to the order of a few nanometers. For the purposes of this study, the model was applied to two different scenarios, each of which involved a different geological formation where the extraction of shale gas is of interest. The results from the simulations performed indicate, as expected, that natural gas production is higher with the use of CO<sub>2</sub> than water, and that the amount of natural gas obtained per tonne of CO<sub>2</sub> injected into the formation is higher. This conclusion coupled with the sequestration of the injected CO<sub>2</sub> underlies the attractiveness of using CO<sub>2</sub> for this purpose. Additional aspects, such as the relatively low viscosity of supercritical CO<sub>2</sub> and thus lower pumping cost, provide further incentive for its use.

#### References

- [1] R.W.J. Edwards, M.A. Celia, K.W. Bandilla, F. Doster, C.M. Kanno, A Model To Estimate Carbon Dioxide Injectivity and Storage Capacity for Geological Sequestration in Shale Gas Wells, Environ. Sci. Technol. 49 (2015) 9222–9229.
- [2] R.W.J. Edwards, M.A. Celia, K.W. Bandilla, F. Doster, C.M. Kanno, A Model To Estimate Carbon Dioxide Injectivity and Storage Capacity for Geological Sequestration in Shale Gas Wells, Environ. Sci. Technol. 49 (2015) 9222–9229.
- [3] M.O. Eshkalak, E.W. Al-Shalabi, A. Sanaei, U. Aybar, K. Sepehrnoori, Simulation study on the CO<sub>2</sub>-driven enhanced gas recovery with sequestration versus the re-fracturing treatment of horizontal wells in the U.S. unconventional shale reservoirs, J. Nat. Gas Sci.

- Eng. 21 (2014) 1015–1024.
- [4] L. Gandossi, An overview of hydraulic fracturing and other formation stimulation technologies for shale gas production, 2013.
- [5] M.L. Godec, GLOBAL TECHNOLOGY ROADMAP FOR CCS IN INDUSTRY - Sectoral Assessment CO<sub>2</sub> Enhanced Oil Recovery, 2011.
- [6] R. Heller, M. Zoback, Adsorption of methane and carbon dioxide on gas shale and pure mineral samples, *J. Unconv. Oil Gas Resour.* 8 (2014) 14–24.
- [7] J. Kim, G.J. Moridis, Numerical analysis of fracture propagation during hydraulic fracturing operations in shale gas systems, *Int. J. Rock Mech. Min. Sci.* 76 (2015) 127–137.
- [8] E.W. Lemmon, M.L. Huber, M.O. McLinden, NIST Standard Reference Database 23: Reference Fluid Thermodynamic and Transport Properties-REFPROP, (2007).
- [9] R.S. Middleton, J.W. Carey, R.P. Currier, J.D. Hyman, Q. Kang, S. Karra, J. Jiménez-Martínez, M.L. Porter, H.S. Viswanathan, Shale gas and non-aqueous fracturing fluids: Opportunities and challenges for supercritical CO<sub>2</sub>, *Appl. Energy.* 147 (2015) 500–509.
- [10] T. Patzek, F. Male, M. Marder, A simple model of gas production from hydrofractured horizontal wells in shales, *Am. Assoc. Pet. Geol. Bull.* 98 (2014) 2507–2529.
- [11] T.W. Patzek, F. Male, M. Marder, Gas Production in the Barnett Shale Obeys a Simple Scaling Theory, *Proc. Natl. Acad. Sci. U. S. A.* 110 (2013) 19731–6.
- [12] P. Pei, K. Ling, J. He, Z. Liu, Shale gas reservoir treatment by a CO<sub>2</sub>-based technology, *J. Nat. Gas Sci. Eng.* 26 (2015) 1595–1606.
- [13] A. Péneloux, E. Rauzy, R. Fréze, A consistent correction for Redlich-Kwong-Soave volumes, *Fluid Phase Equilib.* 8 (1982) 7–23.